

# Selective Association of Outer Surface Lipoproteins with the Lipid Rafts of *Borrelia burgdorferi*

Alvaro Toledo,<sup>a</sup> Jameson T. Crowley,<sup>a\*</sup> James L. Coleman,<sup>a,b</sup> Timothy J. LaRocca,<sup>a\*</sup> Salvatore Chiantia,<sup>c</sup> Erwin London,<sup>c</sup> Jorge L. Benach<sup>a</sup>

Department of Molecular Genetics and Microbiology, Stony Brook University, Stony Brook, New York, USA<sup>a</sup>; New York State Department of Health, Stony Brook University, Stony Brook, New York, USA<sup>b</sup>; Department of Biochemistry and Cell Biology, Stony Brook University, Stony Brook, New York, USA<sup>c</sup>

\* Present address: Jameson T. Crowley, Center for Immunology and Inflammatory Diseases, Harvard University, Boston, Massachusetts, USA; Timothy J. LaRocca, Department of Pediatrics, Columbia University, New York, New York, USA.

**ABSTRACT** *Borrelia burgdorferi* contains unique cholesterol-glycolipid-rich lipid rafts that are associated with lipoproteins. These complexes suggest the existence of macromolecular structures that have not been reported for prokaryotes. Outer surface lipoproteins OspA, OspB, and OspC were studied for their participation in the formation of lipid rafts. Single-gene deletion mutants with deletions of  $\Delta ospA$ ,  $\Delta ospB$ , and  $\Delta ospC$  and a spontaneous gene mutant, strain B313, which does not express OspA and OspB, were used to establish their structural roles in the lipid rafts. All mutant strains used in this study produced detergent-resistant membranes, a common characteristic of lipid rafts, and had similar lipid and protein slot blot profiles. Lipoproteins OspA and OspB but not OspC were shown to be associated with lipid rafts by transmission electron microscopy. When the ability to form lipid rafts in live *B. burgdorferi* spirochetes was measured by fluorescence resonance energy transfer (FRET), strain B313 showed a statistically significant lower level of segregation into ordered and disordered membrane domains than did the wild-type and the other single-deletion mutants. The transformation of a B313 strain with a shuttle plasmid containing *ospA* restored the phenotype shared by the wild type and the single-deletion mutants, demonstrating that OspA and OspB have redundant functions. In contrast, a transformed B313 overexpressing OspC neither rescued the FRET nor colocalized with the lipid rafts. Because these lipoproteins are expressed at different stages of the life cycle of *B. burgdorferi*, their selective association is likely to have an important role in the structure of prokaryotic lipid rafts and in the organism's adaptation to changing environments.

**IMPORTANCE** Lipid rafts are cholesterol-rich clusters within the membranes of cells. Lipid rafts contain proteins that have functions in sensing the cell environment and transmitting signals. Although selective proteins are present in lipid rafts, little is known about their structural contribution to these domains. *Borrelia burgdorferi*, the agent of Lyme disease, has lipid rafts, which are novel structures in bacteria. Here, we have shown that the raft-associated lipoproteins OspA and OspB selectively contribute to lipid rafts. A similar but non-raft-associated lipoprotein, OspC, cannot substitute for the role of OspA and OspB. In this study, we have demonstrated that lipoprotein association with lipid rafts is selective, further suggesting a functional adaptation to different stages of the spirochete life cycle. The results of this study are of broader importance and can serve as a model for other bacteria that also possess cholesterol in their membranes and, therefore, may share lipid raft traits with *Borrelia*.

Received 4 February 2014 Accepted 10 February 2014 Published 11 March 2014

**Citation** Toledo A, Crowley JT, Coleman JL, LaRocca TJ, Chiantia S, London E, Benach JL. 2014. Selective association of outer surface lipoproteins with the lipid rafts of *Borrelia burgdorferi*. mBio 5(2):e00899-14. doi:10.1128/mBio.00899-14.

**Editor** Liise-anne Pirofski, Albert Einstein College of Medicine

**Copyright** © 2014 Toledo et al. This is an open-access article distributed under the terms of the [Creative Commons Attribution-Noncommercial-ShareAlike 3.0 Unported license](https://creativecommons.org/licenses/by-nc-sa/3.0/), which permits unrestricted noncommercial use, distribution, and reproduction in any medium, provided the original author and source are credited.

Address correspondence to Jorge L. Benach, Jorge.benach@stonybrook.edu.

*Borrelia burgdorferi* is the causative agent of Lyme disease (1, 2) and affects the skin, heart, joints, and nervous system (3). *B. burgdorferi* has outer and inner membranes, and the flagella occupy the periplasmic space (4). The outer membrane of *Borrelia* contains phosphatidylcholine and phosphatidylglycerol, numerous lipoproteins (5–9), and three glycolipids, two of which contain cholesterol. These glycolipids were identified as cholesteryl 6-*O*-acyl- $\beta$ -D-galactopyranoside or cholesteryl 6-*O*-palmitoyl- $\beta$ -D-galactopyranoside (ACGal/Bb-GL-I), cholesteryl- $\beta$ -D-galactopyranoside (CGal), and mono- $\alpha$ -galactosyl-diacylglycerol (MGalD) (10–12). Although there are some exceptions, such as

*Helicobacter*, *Mycoplasma*, *Ehrlichia*, *Anaplasma*, and *Brachyspira* species (13–17), the presence of cholesterol and cholesterol glycolipids in prokaryotes is unusual. Functional lipid microdomains that do not have cholesterol but have prokaryotic homologs of Flotillin-1 (a major component of eukaryotic lipid rafts) have been described for other bacteria (18). In eukaryotic cell membranes, sterols form lipid rafts that are ordered areas that are rich in lipid-anchored proteins (19, 20). Lipid rafts are important for receptor clustering and lateral sorting of proteins (21, 22), as well as elasticity, endocytosis, exocytosis, and vesicle formation and budding (23–26).

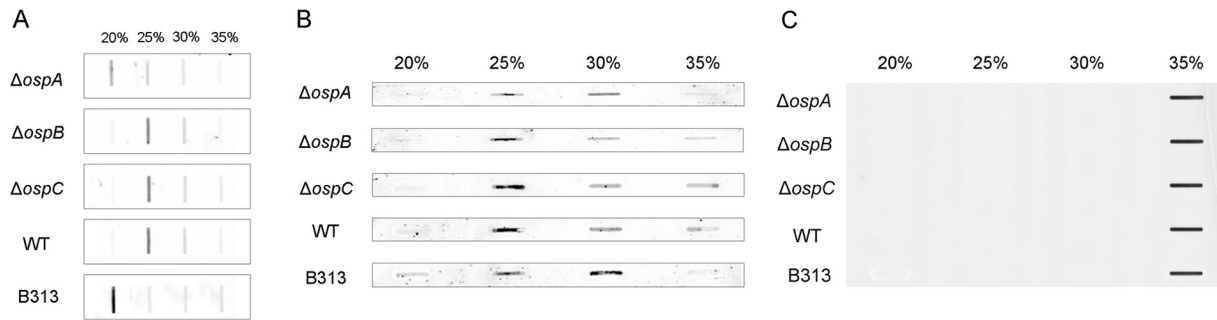


**FIG 1** Slot blot analysis of gradient fractions of *B. burgdorferi* wild type (WT), single *osp* mutants, and B313 obtained after whole spirochetes were subjected to Triton X-100 treatment at 4°C overnight and separated by an iodixanol density gradient. Membranes were probed with a rabbit polyclonal antibody to asialo GM1 (A), rabbit polyclonal antibody to HtrA (B), and mouse monoclonal antibody to DnaK (C). Primary antibodies were followed by goat anti-rabbit IgG IR800 (A, B) and anti-mouse IgG IR800 (C).

Recently, we demonstrated that cholesterol glycolipids form lipid rafts in *B. burgdorferi* (27, 28). Moreover, we showed the impact of different sterols in lipid raft formation in *B. burgdorferi* and the ability of the spirochete to process these sterols and to form glycolipids (28). However, little is known about the contribution of proteins to the formation and dynamics of the lipid rafts. It is possible that proteins could influence the raft formation, especially as large numbers of lipoproteins are abundant in the membranes of this spirochete (29). Many of these lipoproteins occur in the outer membrane and have domains that can be detected on the surface by microscopy and by limited proteolysis. These lipoproteins are known as outer surface proteins (Osp). OspA and OspB occupy prominent bands (31 and 34 kDa, respectively) in the electrophoretic profile of cultured *B. burgdorferi* and are cationic (30, 31). In addition to their expression in culture, OspA and OspB are expressed in the unfed tick, but they are not expressed in the mammalian host (32). OspA was used as the molecular subunit of a vaccine for Lyme disease (33–35) and also functions as an adhesin in the tick midgut (36). OspB is the target of an unusual class of bactericidal antibodies (37–39). OspC is an enigmatic variable lipoprotein that begins to be expressed during the acquisition of blood by the nymphal tick and in the early stages of infection in the mammal host (40, 41). OspC is a potential vaccinogen (42, 43), is used as a marker for human infection (44, 45), and is a receptor for plasminogen (46–48).

We have documented the colocalization of OspB with the lipid rafts on the membrane of *B. burgdorferi* by microscopy, as well as documenting the coisolation of OspA and OspB in detergent resistance membranes (DRM) derived from *B. burgdorferi* membranes (27), which is often a measure of raft association. Here, we analyze the impacts that OspA, OspB, and OspC, as principal constituents of such structures, have on the genesis and dynamics of the lipid rafts.

## RESULTS

We previously showed that lipoproteins OspA and OspB partition preferentially in DRM and that OspC is present in small quantities (27). OspA and OspB were chosen for experiments to determine the role of lipoproteins in the formation of lipid rafts because of their abundance in the DRM fractions and because we have shown previously, using transmission electron microscopy (TEM), that OspB is associated with the lipid rafts formed by the cholesterol glycolipids of *B. burgdorferi* (27). OspC was also chosen, because

this lipoprotein is upregulated in the nymphal-tick blood-feeding stage and is required for the early stages of mammalian infection (40, 41, 49). In addition, lipid rafts are important for budding and vesicle formation (24) and lipoproteins OspA to -D are the most frequent constituents of multiprotein complexes of the outer membrane vesicles that bud off of *B. burgdorferi* cells (50, 51).

**All single- and multiple-deletion mutants had DRM.** Thin-layer chromatography (TLC) of single- and multiple-deletion mutants showed identical lipid profiles (see Fig. S1 in the supplemental material). Anti-asialo GM1 antibody was shown previously to cross-react with *Borrelia* cholesterol glycolipids and has been used to detect lipid rafts in *B. burgdorferi* in previous studies (27, 28, 52). Cholesterol glycolipids from all mutants and the wild type (WT) partitioned in the DRM fractions (20 to 30% iodixanol) (Fig. 1A). There were some differences in the slot blot profiles among the mutants. Cholesterol glycolipids partitioned into the 25% iodixanol fraction for the  $\Delta ospB$ ,  $\Delta ospC$ , and WT strains, between the 20% and 25% fractions for the  $\Delta ospA$  mutant, and in the 20% iodixanol fraction for B313. The differences in flotation in the lipid raft fractions could be due to lower densities of the  $\Delta ospA$  mutant and B313 DRM, which lack the highly abundant OspA. HtrA, a serine protease (53), was used as a marker for lipid raft integrity because this protease partitioned almost exclusively in the lipid raft fractions. Most of the HtrA was present in the DRM fractions (20 to 30%), confirming its association with lipid rafts in all mutant and WT strains used (Fig. 1B). Only small amounts of HtrA could be found in the soluble fraction (35%). DnaK (Fig. 1C) was used as a control, since it is not associated with lipid raft proteins and partitions in the soluble fraction.

**OspA and OspB but not OspC colocalized with lipid rafts.** TEM with negative staining of WT *B. burgdorferi*, grown under normal conditions (33°C), showed colocalization of OspA with lipid rafts visualized with colloidal gold (Fig. 2A). We obtained similar results using OspB, confirming previous reports showing colocalization with lipid rafts (27) (Fig. 2B). The ultrastructural results with OspA and OspB are concordant with the data obtained by slot blots of DRM. OspC did not colocalize with the cholesterol glycolipids (Fig. 2C) under various culture conditions (33°C or 35°C and pH 6.7 to induce expression of OspC).

**Clusters of lipid rafts were confirmed in WT,  $\Delta ospA$ ,  $\Delta ospB$ ,  $\Delta ospC$ , and B313 strains by qualitative and quantitative ultrastructural analysis.** To determine if there were any differences in the distribution of the 6-nm colloidal gold particles (anti-asialo

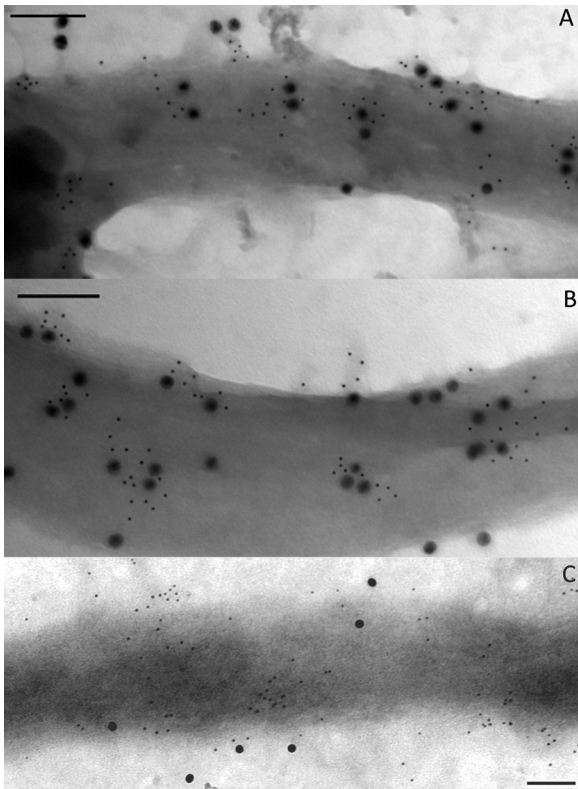


**FIG 2** TEM image shows colocalization of lipoproteins and lipid rafts on the membrane of *B. burgdorferi* cells labeled with a murine monoclonal antibody to OspA (A) OspB (B), or OspC (C) and rabbit polyclonal antibody to asialo GM1, followed by antibody to mouse IgG and to rabbit IgG conjugated with 18-nm and 6-nm colloidal gold, respectively. Bars = 100 nm.

GM1 antibody), the spirochetes were examined for the presence of clusters by TEM. The WT and all mutant strains had similar distributions of clusters of colloidal gold particles (Fig. 3A to E). Based on the ultrastructural results, there were no differences in the distribution of lipid raft clusters on the membranes of WT and mutant *B. burgdorferi* strains. Quantitative comparisons were obtained using an analytical approach with Ripley's  $K$  function. The analytical results for clustering of lipid rafts were in agreement with the visual assessment of ultrastructure, with positive clustering [ $L(r) - r$ ] values above the 95% confidence limit (Fig. 3F).

**Single-deletion *osp* mutants and the WT had similar levels and stabilities of ordered/disordered domain segregation.** Given that there were no biochemical (Fig. 2A and B) or ultrastructural (Fig. 3A to F) differences in the composition and clustering of lipid rafts among single *osp* mutants and WT *B. burgdorferi*, we carried out fluorescence resonance energy transfer (FRET) analysis in live spirochetes using two probes, 1-(4-trimethylammoniumphenyl)-6-phenyl-1,3,5-hexatriene *p*-toluenesulfonate (TMA-DPH [donor]) and octadecyl rhodamine B chloride (ODRB [acceptor]). TMA-DPH has a moderate affinity for ordered domains, while ODRB has a high affinity for disordered domains. The coexistence of ordered and disordered domains in a membrane is detected as weak FRET, i.e., a high value of residual donor fluorescence in the presence of the acceptor (measured as the ratio of fluorescence intensity with acceptor to that without acceptor [ $F/F_o$ ]) (54). Donor fluorescence in the presence of the acceptor decreases as the temperature increases due to the melting of ordered domains at high temperatures, which in turn results in increased proximity between donor and acceptor. When donor fluorescence ( $F/F_o$ ) in the FRET assay was measured as a function of increasing temperature, the WT had  $F/F_o$  ratios similar to those of the  $\Delta ospA$ ,  $\Delta ospB$ , and  $\Delta ospC$  mu-

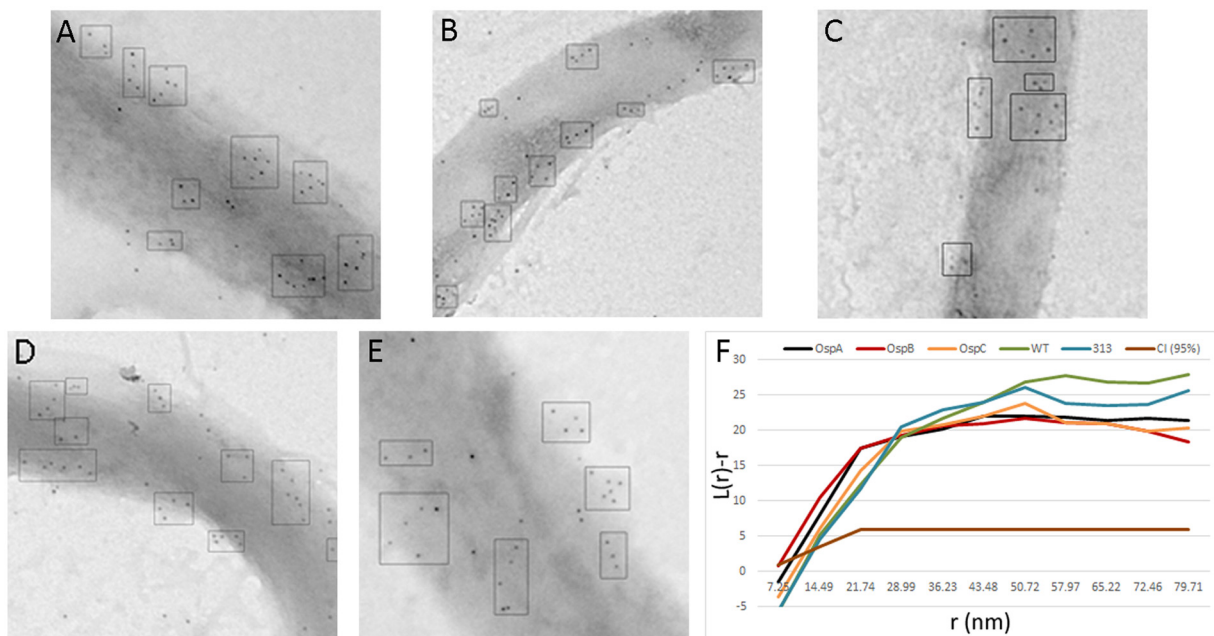


**FIG 3** *B. burgdorferi* WT and single *osp* mutants form lipid raft clusters. (A to E) TEM images of lipid raft clusters on the surface of  $\Delta ospA$  (A),  $\Delta ospB$  (B),  $\Delta ospC$  (C), B313 (D), and WT (E) cells were probed with rabbit polyclonal antibody to asialo GM1, followed by an antibody to rabbit IgG conjugated with colloidal gold (6 nm). Bars = 100 nm. (F) Statistical analysis of the gold particle distribution on the surface of *B. burgdorferi* using Ripley's  $K$  function. The confidence index (CI) was estimated by simulating 100 random particles.



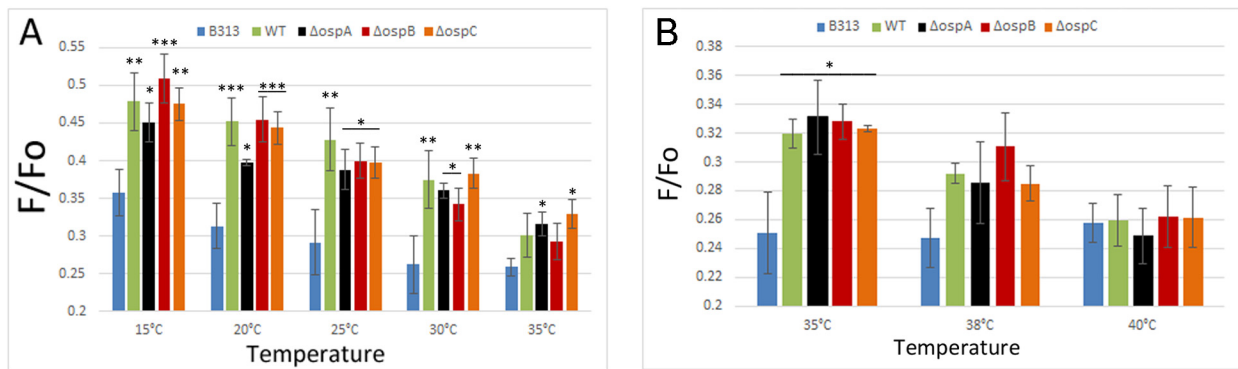


**FIG 4** Fluorescence resonance energy transfer on live cells of *B. burgdorferi* WT, B313,  $\Delta ospA$ ,  $\Delta ospB$ , and  $\Delta ospC$  strains was measured using TMA-DPH (donor) and ODRB (acceptor) probes. Shown are  $F/F_o$  ratios as a function of temperature from 15°C to 35°C (A) or 35°C to 40°C (B) for the indicated strains.  $P$  values for the differences between B313 FRET values and those of the other strains are indicated as follows: \*,  $P < 0.05$ ; \*\*,  $P < 0.01$ ; \*\*\*,  $P < 0.001$ .

tants (Fig. 4A). The  $F/F_o$  ratios for all strains at all temperatures tested were not statistically different.

**Multiple *osp* mutant B313 had a significantly reduced membrane order that was restored to wild-type levels in B313-pBOA-1.** Strain B313, which does not express OspA and OspB (Fig. 5), had a significantly decreased level of domain segregation compared to the results for the WT,  $\Delta ospA$ ,  $\Delta ospB$ , or  $\Delta ospC$  strain (Fig. 4A). At 15°C, the  $F/F_o$  ratio of B313 was significantly reduced relative to those of the other strains, and at higher temperatures,  $F/F_o$  decreased until it reached a minimum at 30°C. In contrast, the other strains started at higher  $F/F_o$  ratios at 15°C (0.45 to 0.50), which gradually decreased as a function of the temperature but did not reach a minimum in the temperature range studied.

The FRET experiments were repeated to determine  $F/F_o$  as a function of temperature from 35°C to 40°C. The  $F/F_o$  ratios of B313 did not decrease with an increase in temperature (Fig. 4B), indicating that increasing temperature in this range did not alter domain properties, either because domains no longer existed or because they were too small to be detected by FRET. In contrast, above 35°C, the WT and the other single *osp* mutants exhibited decreased  $F/F_o$  ratios at higher temperatures, displaying increasing loss of detectable domain formation up to at least 40°C. At 40°C, the  $F/F_o$  values for the B313 and other strains became similar, suggesting that they had similar levels of domain formation.

To demonstrate that the decreased  $F/F_o$  ratios (i.e., stronger FRET) observed in B313 were due to the simultaneous lack of the

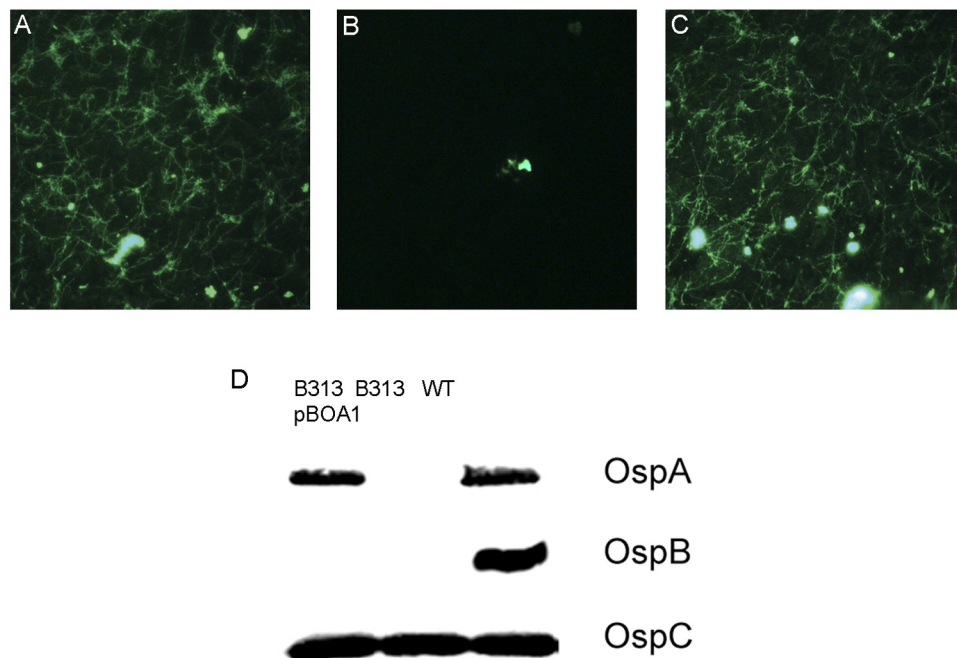


**FIG 5** *B. burgdorferi* B313-pBOA-1 produces OspA, which is expressed on the surface. (A to C) Immunofluorescence assay images showing surface localization of OspA on WT (A), B313 (B), and B313-pBOA-1 (C) cells, all using the same exposures for microscope settings. (D) Western blot analysis of OspA, OspB, and OspC in WT, B313, and B313-pBOA-1 strains.

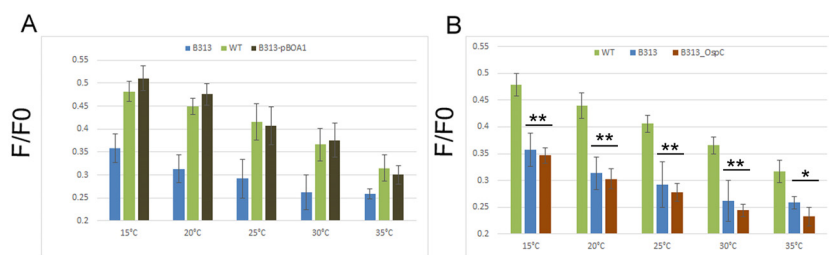


**FIG 6** Fluorescence resonance energy transfer on live *B. burgdorferi* cells of the indicated strains was measured using TMA-DPH (donor) and ODRB (acceptor) probes. Shown are  $F/F_0$  ratios as a function of temperature. \*,  $P < 0.05$ ; \*\*,  $P < 0.01$ ; \*\*\*,  $P < 0.001$ .

lipoproteins OspA and OspB, we transformed B313 with *ospA* under the control of its native promoter using the shuttle vector pKFSS1. The resulting transformant, named B313-pBOA-1, has the same plasmid profile as the parental strain B313. The parental strain B313 used for the transformations lacks the major lipoproteins OspA, -B, and -D due to the absence of plasmids lp38 (carrying *ospD*) and lp54 (carrying *ospA* and *ospB*), but it has cp26, which carries *ospC*. B313-pBOA-1 produced OspA at levels similar to those in the wild-type strain, and the OspA localized on the surface, as determined by immunofluorescence assay (IFA) (Fig. 5A to C) and immunoblotting (Fig. 5D).

The FRET experiments were repeated with the transformant B313-pBOA-1. The results showed that the  $F/F_0$  fluorescence ratio was restored to WT levels and that it decreased with increasing temperatures similarly to the WT values (Fig. 6A). These results indicate that the decreased ratio observed in B313 reflects the simultaneous lack of both OspA and OspB and can be restored with the expression of just one of the lipoproteins (OspA), demonstrating redundant functions of OspA and OspB in lipid raft organization. A transformant with the control plasmid pKFSS1 did not express OspA, and the FRET values did not change.

**Multiple *osp* mutant B313 has a significantly reduced membrane order that is not restored to wild-type levels by overexpression of OspC.** To determine whether overexpression of OspC could restore FRET to wild-type levels, we transformed B313 with the pBSV2G-*ospC* plasmid. OspC overexpression in this transformant was shown by the electrophoretic profiles and by immunoblotting (see Fig. S2A and B in the supplemental material). The transformation of B313 with pBSV2G-*ospC* plasmid resulted in the overexpression of OspC but did not change its localization. This indicates that OspC is not associated with lipid rafts in any stage of the *B. burgdorferi* life cycle. The level of domain segregation in the transformant was measured by FRET. The results showed that the  $F/F_0$  fluorescence ratio was similar to that of B313 and was significantly lower than the WT ratio (Fig. 6B). These results indicated that the decreased ratio observed in B313 was due to the lack of lipid raft-associated lipoproteins and could not be restored by the overexpression of a nonraft lipoprotein at very high levels, demonstrating that raft-associated proteins are important for lipid raft formation.

## DISCUSSION

The presence of lipid groups increases the hydrophobic properties of proteins. Acylation of proteins promotes their association with membranes and, specifically, their ability to be a part of lipid-ordered microdomains (lipid rafts). This structural arrangement has never been demonstrated in prokaryotes. In this study, our

most compelling finding is that lipoproteins selectively affect lipid raft formation, proving that raft-associated proteins can modify their environment. In addition, we demonstrated that acylation is not the only requirement for protein-raft association. Lipid rafts are macromolecular complexes rich in cholesterol that contains a subset of selected proteins and that represents a unique structure among the prokaryotes. Lipid rafts in *Borrelia* reveal a level of structural and, possibly, functional sophistication thus far unexpected in bacteria. In addition, and specifically for *Borrelia*, we have demonstrated that there is selectivity to lipoprotein association with lipid rafts, further suggesting a functional adaptation to different stages of the spirochete life cycle.

We previously demonstrated that *B. burgdorferi* has eukaryotic-like lipid rafts with cholesterol glycolipids and that the type of sterol present in *B. burgdorferi* is key to their formation (27, 28). In this study, by using a novel FRET technique with live organisms, we showed that lipid raft-associated lipoproteins also contribute to these structures. The use of live organisms offers a marked advantage over experiments using passive membrane models composed of isolated lipids. To study the importance of proteins in the formation of lipid rafts, we compared a WT strain to single-deletion mutant strains with deletions of the major raft-associated lipoproteins OspA and OspB and a non-raft-associated protein, OspC, and a double mutant, B313, that lacks both raft-associated proteins (OspA and -B). All of the *Borrelia* mutants tested had the same lipid profile by TLC, showing the presence of cholesterol and cholesterol glycolipids that are needed for lipid raft formation. In addition, the ultrastructural data showed that all of the mutants had similar lipid raft domains. Therefore, these data suggest that the cholesterol and cholesterol glycolipids in *Borrelia* are sufficient for lipid raft formation.

However, when we used a more sensitive approach, FRET with live spirochetes, the spontaneous mutant B313 (55), which does not express the raft-associated lipoproteins OspA and OspB, had a significantly increased FRET compared to those of the WT and single lipoprotein mutants. Also, FRET reached a maximum at a lower temperature in B313 than in the WT and single mutant strains. These results are consistent with the presence of fewer or smaller lipid raft domains in the B313 strain. Based on previous studies showing strong FRET being associated with loss of lipid microdomain formation in *B. burgdorferi* (28), there is likely to be a complete loss of domain formation at the temperature at which FRET reaches a maximum.

The transformant B313-pBOA-1 expressed OspA (under its native promoter) in the membrane at a level similar to the WT level and had FRET values similar to those of the WT and single mutants. Moreover, a higher FRET was detected only in B313 and

not in the single *osp* mutants. This demonstrated that the B313 phenotype was due to the lack of both of the raft-associated lipoproteins, indicating that lipoproteins affect the formation of lipid rafts and have active roles in their formation. Also, this suggests that the abundance of the raft-associated lipoproteins might be more important than the type of protein itself, since the contributions of lipoproteins OspA and OspB to lipid rafts seem to be redundant. Also, the fact that the single *ospA/ospB* mutants, the WT, and B313-pBOA-1 had similar FRET values suggests that lower combined amounts of OspA/OspB than are present in the WT are sufficient for maximum domain formation.

However, despite the redundancy of OspA and OspB, not all lipoproteins associate with lipid rafts. The overexpression of OspC (under the *flaB* promoter) did not result in restoring FRET values to those of the WT or the single lipoprotein mutants, suggesting that association with lipid rafts is selective. These FRET results and the lack of colocalization of OspC as found by TEM make a convincing case that there is no association of this lipoprotein with lipid rafts. All three lipoproteins (OspA, -B, and -C) have acyl chains that are the most likely domains for association with the lipid rafts. Furthermore, all three form ligand binding pockets that could potentially bind small molecules, such as cholesterol glycolipids (27). Despite these similarities, however, OspC is quite different from OspA/-B in that it forms a homodimer and has a strong alpha-helical structure and a negatively charged cap (56, 57). These biophysical differences could potentially account for the lack of association of OspC with the lipid rafts.

The physiological functions of OspA and OspB are not known, but they have essential roles in colonization in the tick stage. OspA anchors in the outer leaflet of the outer membrane through the involvement of a BamA ortholog (58, 59). To the extent that OspA and OspB are associated with the lipid rafts, it would follow that this association is important throughout the tick stage of *B. burgdorferi*. As part of the lipid rafts, OspA and OspB could have a stabilizing function in the membrane of this spirochete in the low-temperature and nutrient-deficient environment of the tick midgut. The participation of OspB in membrane integrity has been demonstrated by its susceptibility to attack by bactericidal antibodies (27, 37, 38).

In contrast, OspC did not show colocalization with lipid rafts in culture, even when it was overexpressed. OspC is induced during the blood meal and in the course of early infection of mammals (40, 60) but is not required for later stages (41, 61). It has been proposed that there is a succession of functionally equivalent proteins that are sequentially expressed at various stages of infection (62, 63). This is an intriguing model to test whether lipoproteins uniquely present at different stages of infection perform the same function in the context of lipid rafts. However, from our results, we conclude that this sequence of lipoprotein expression may not be tied to inclusion in the lipid raft complex.

Lipid rafts are dynamic structures that are temperature sensitive. Mouse-derived spirochetes show fewer lipid rafts, and those present are highly packed (27). At temperatures above 35°C, all of the strains tested showed high FRET values, suggesting that the role of OspA and OspB is critical at low temperatures (tick) but not at high temperatures (mammal), when other lipoproteins, such as OspC, that are not raft related are expressed. The selective association of lipoproteins with lipid rafts could reflect their behavior *in vivo* and provide insights into their structure and function.

The identification of lipoproteins that associate selectively with lipid rafts further suggests that the membrane of spirochetes has structures that are functionally equivalent to those of eukaryotic lipid rafts. This type of membrane organization is novel and unexpected in the eubacteria. The presence of these lipoprotein-lipid raft complexes could represent membrane platforms that segregate proteins that function at different stages of infection. Thus, the integrity of these complexes could be essential for promoting or inhibiting the physiological processes that are related to adaptation to the different hosts.

Our findings also have broader significance to microbiology in that the presence of cholesterol and cholesterol glycolipids in prokaryotic membranes is increasingly being recognized in many genera of bacteria. Thus, the presence of similar lipid rafts in other bacterial pathogens is very likely. The knowledge obtained about *Borrelia* lipid rafts will be immediately applicable to other pathogens that share cholesterol-protein complexes. The structure of prokaryotic lipid rafts is a virtually unknown area of investigation with broad applicability to bacteriology and to studies on the evolution of these membrane microdomains.

## MATERIALS AND METHODS

**Bacteria, cultures, and antibodies.** Different strains and mutants of *B. burgdorferi* (see Table S1 in the supplemental material) (41, 64) were grown in BSK-II supplemented with 6% rabbit serum (Sigma) at 33°C and, for some experiments, at pH 6.7 at 35°C. Murine IgG1 monoclonal antibodies to OspA (65) and OspB (66), murine and rabbit polyclonal antibodies to OspC (67) and asialo GM1 (Abcam), and rabbit polyclonal antibody to HtrA (68) were used for different procedures. Mouse and rabbit antibodies to OspC were generated from a recombinant construct made from plasmid pET46 LIC, provided by Richard T. Marconi (Virginia Commonwealth University). The  $\Delta ospA$  and  $\Delta ospB$  mutants were provided by Thomas Schwan, and the  $\Delta ospC$  and B313 strains were provided by Patricia Rosa (both from the Rocky Mountain Laboratories, NIH). Plasmid pBSV2G-*ospC* was also provided by Patricia Rosa (41), and plasmid pKFSS1 was provided by Scott Samuels from the University of Montana (69).

**Detection methods for lipids.** Lipids from *B. burgdorferi* were extracted using chloroform-methanol (1:2) (70) and were spotted on a high-performance TLC silica plate (EM Separations), followed by resolution with a chloroform-methanol (85:15) mobile phase, drying, and staining with iodine vapor. The standards included phosphatidylcholine, phosphatidylglycerol (Avanti Polar Lipids), and cholesterol (Sigma). Known  $R_f$  values from identical solvent systems (11, 12) were also used to determine lipid identity.

**Isolation, detection, and analysis of DRMs of *B. burgdorferi*.** DRMs were isolated from WT and mutant strains of whole *B. burgdorferi* by detergent insolubility using Triton X-100, followed by gradient separation using the caveola/raft isolation kit (Sigma) (27). Fractions were diluted in phosphate-buffered saline (PBS; Gibco), applied to nitrocellulose in a PR-648 slot blot apparatus (Hoefer), and blocked with 2% casein in PBS. The primary antibodies included a rabbit polyclonal IgG against asialo GM1 for cholesterol glycolipids and rabbit anti-HtrA protease antibody as markers for the DRM fractions and murine IgG1 monoclonal antibody to DnaK as a control for the soluble fraction (65). The secondary antibodies used were anti-rabbit IgG IR800 conjugate (Rockland Immunochemicals) for anti-asialo GM1 and anti-HtrA antibodies and anti-mouse IgG IR800 conjugate for DnaK. All slot blots were read in an Odyssey scanner (Li-Cor Biosciences) in the 800-nm channel.

**FRET measurements of live *B. burgdorferi* cells.** The fluorescent probes used for FRET measurements, 1-(4-trimethylammoniumphenyl)-6-phenyl-1,3,5-hexatriene *p*-toluenesulfonate (TMA-DPH) (Invitrogen) and octadecyl rhodamine B (ODRB) (Invitrogen), were stored in ethanol at -20°C, and concentrations determined by absorbance using  $\epsilon =$



84,800 M<sup>-1</sup> cm<sup>-1</sup> at 353 nm and 125,000 M<sup>-1</sup> cm<sup>-1</sup> at 555 nm, respectively. FRET measurements were made on a PCI photon counting fluorometer (ISS, Inc.) using quartz semimicrocuvettes. FRET between the donor, TMA-DPH, and the acceptor, ODRB, in live spirochetes was calculated from TMA-DPH fluorescence at an excitation wavelength of 352 nm and an emission wavelength of 430 nm. Briefly, 2.1 μl of TMA-DPH (from a 175 μM stock solution) was added to 4 ml of spirochetes at a concentration of 4 × 10<sup>8</sup> cells/ml and incubated at room temperature for 10 min. The cells were divided into four 900-μl aliquots. Two of the aliquots were defined as Fo samples, and for the other two aliquots (F samples), 5.2 μl of ODRB (322 μM stock solution) was added, followed by incubation at 35°C for 15 min. The ratio of fluorescence intensity with acceptor to that without acceptor ( $F/F_o$ ) was calculated (after subtraction of background values from samples prepared without TMA-DPH) as a function of decreasing temperature for every 5°C from 35°C to 15°C or each 2.5°C from 40°C to 35°C. Spirochetes subjected to the procedures described above were returned to BSK medium to determine growth and viability.

**Transmission electron microscopy.** Spirochetes were fixed to polyvinyl formal-coated grids (Ted Pella) using 1% glutaraldehyde (Sigma) (38). For the detection of lipoproteins, murine monoclonal antibodies to OspA and to OspB and murine polyclonal serum to OspC in 1% bovine serum albumin (BSA) were added to the fixed spirochetes. Goat antibody to mouse IgG conjugated to 18-nm colloidal gold (Jackson Immunochemicals) in 1% BSA was added to the grids for 1 h, followed by 3 washes with PBS. Cholesterol glycolipids were detected by probing grids with rabbit antibody to asialo GM1 (rabbit polyclonal IgG; AbCam) in 1% BSA for 1 h. This was followed by detection with goat anti-rabbit IgG conjugated to 6-nm colloidal gold (Jackson Immunochemicals) in 1% BSA for 1 h and then by 3 washes with PBS. Antibody binding was followed by staining with 0.5% phosphotungstic acid (PTA; negative stain) for 35 s as described previously (38). Controls for all TEM procedures included experiments with irrelevant isotype-matched antibodies and with secondary colloidal gold-conjugated antibodies without primary antibodies.

The distribution of gold particles bound to the rabbit anti-asialo GM1 antibody in the TEM micrographs was analyzed using the common linear transformation of Ripley's *K* function for an analytical assessment of clustering (71–73). Briefly, TEM images of *B. burgdorferi* were cropped to include only the largest straight cropped image possible, and a total of 15 random images per condition were analyzed. All the images were subjected to a computational analysis using self-written MatLab algorithms. The positions of the particles were highlighted manually on the images, and a script assigned them *x/y* coordinates. To avoid edge effects, we only included particles that were >80 nm away from the edge of the image. These *x/y* coordinates were analyzed with a MatLab script using the following formula for transformation of Ripley's *K* function:

$$L(r) - r = \sqrt{\frac{N(r)}{D\pi}} - r = \sqrt{\frac{K(r)}{\pi}} - r$$

where *N*(*r*) is the number of particles within a radius *r* of a given particle and *Dπ* is the average particle surface. *L*(*r*) - *r* measures whether clustering exists. It reflects the excess of particles within a circular region with a radius *r* centered on any given particle compared to a random distribution. *L*(*r*) - *r* will be within zero ± confidence index (CI) for particles with a random distribution and will be positive for clustering particles. The CI was estimated by simulating 100 random particle distributions and calculating the *L*(*r*) - *r* value for each one.

**Expression of OspA in B313.** The *ospA* gene, including its native promoter, was amplified using the primers OspAF (5' GTCTGCATGCTAT TTGTTATTTGTTAATC 3') and OspAR (5' TCTCGTCTGACTTATTTT AAAGCGTTTTT 3'), which introduced restriction sites for the enzymes SphI and SalI. The amplicon was purified and cloned into the pKFSS1 plasmid (69), provided by Scott Samuels (University of Montana), to create pBOA-1. *E. coli* DH5α (Invitrogen) was transformed with pBOA-1 and plated in LB agar containing 10 μg/ml of streptomycin. Plasmids

from *E. coli* DH5α colonies were purified and screened for the presence of *ospA* to confirm the presence of pBOA-1 by PCR.

*B. burgdorferi* strain B313, an avirulent clone of strain B31 that lacks both OspA and OspB but not OspC, was electroporated with 1 μg of plasmid DNA and plated in semisolid medium and in liquid BSK-II. Transformants were selected with 80 μg/ml of streptomycin. The presence of OspA was confirmed by indirect immunofluorescence and by immunoblotting. The plasmid profile remained unaltered after transformation of B313. Transformants with the empty vector, pKFSS1, were also made as described above.

**Overexpression of OspC in B313** To overexpress OspC in B313, spirochetes were electroporated with 1 μg of the pBSV2G-*ospC* plasmid containing the gene for OspC under the *flaB* promoter (41). Gentamicin-resistant transformants were screened for plasmid content, and one of the clones was selected for comparison of OspC production with that of B313. Overproduction of OspC by B313 containing the pBSV2G-*ospC* plasmid was confirmed by electrophoresis and immunoblotting.

**Immunoblots** Each sample, containing a total of 10<sup>6</sup> bacteria, was resuspended in 20 μl of PBS and received 10 μl of 3× SDS-PAGE sample buffer with 2-mercaptoethanol, followed by boiling for 5 min. Each sample was separated by electrophoresis (12.5% SDS-PAGE), and the proteins were transferred to nitrocellulose membranes (GE Healthcare). Murine monoclonal antibodies were used to detect OspA and OspB, whereas OspC was detected by a rabbit polyclonal antiserum. The immunoblots were resolved with goat anti-rabbit IgG IR800 and goat anti-mouse IgG IR800 and visualized by examination with an Odyssey imaging system. For slot blots, the gradient fractions from WT, Δ*ospA*, Δ*ospB*, Δ*ospC*, and B313 strains were analyzed with anti-asialo GM1 antibody and anti-HtrA antibody as described above.

**Immunofluorescence.** IFA was performed to show that *B. burgdorferi* B313-pBOA-1 expressed OspA in the outer membrane. Briefly, *B. burgdorferi* was harvested from the mid-log-phase culture, washed with cold PBS (Invitrogen), and incubated in Hank's balanced salt solution (HBSS) (Invitrogen) with mouse anti-OspA antibody at 35°C for 1 h. After being washed in cold PBS, the spirochetes were added to the wells of Teflon-coated slides (Erie Scientific), dried at 33°C, and fixed in 100% methanol. Goat anti-mouse IgG conjugated to fluorescein isothiocyanate (FITC) (Abcam) was added to each well, followed by incubation for 1 h in a wet chamber. Slides were washed with PBS and mounted with slow-fade medium (Invitrogen). Slides were viewed with a Nikon Eclipse E600 microscope equipped with a super-high-pressure mercury lamp.

**Statistics.** Data were analyzed using analysis of variance and the Tukey-Kramer multiple comparison test with the GraphPad InStat 3.10 statistical program (GraphPad Software, Inc.).

## SUPPLEMENTAL MATERIAL

Supplemental material for this article may be found at <http://mbio.asm.org/lookup/suppl/doi:10.1128/mBio.00899-14/-/DCSupplemental>.

Figure S1, TIF file, 2.7 MB.

Figure S2, TIF file, 22.1 MB.

Table S1, DOCX file, 0.1 MB.

## ACKNOWLEDGMENTS

We are grateful to Patricia Rosa and Thomas Schwan for providing the Δ*ospA*, Δ*ospB*, and Δ*ospC* mutants and strain B313. Richard Marconi generously provided pET46LIC. Scott Samuels provided the pKFSS1 plasmid. We thank David Thanassi for his valuable comments on the manuscript.

This work was supported by NIH grants AI-027044 to J.L.B., GM-099892 to E.L., and Northeast Biodefense Center grant U54-AI-057158 (Lipkin) to A.T.

## REFERENCES

- Burgdorfer W, Barbour AG, Hayes SF, Benach JL, Grunwaldt E, Davis JP. 1982. Lyme disease—a tick-borne spirochetosis? *Science* 216: 1317–1319. <http://dx.doi.org/10.1126/science.7043737>.

2. Benach JL, Bosler EM, Hanrahan JP, Coleman JL, Habicht GS, Bast TF, Cameron DJ, Ziegler JL, Barbour AG, Burgdorfer W, Edelman R, Kaslow RA. 1983. Spirochetes isolated from the blood of two patients with Lyme disease. *N. Engl. J. Med.* 308:740–742. <http://dx.doi.org/10.1056/NEJM198303313081302>.
3. Johnson RC. 1977. The Spirochetes. *Annu. Rev. Microbiol.* 31:89–106. <http://dx.doi.org/10.1146/annurev.mi.31.100177.000513>.
4. Charon NW, Goldstein SF, Marko M, Hsieh C, Gebhardt LL, Motaleb MA, Wolgemuth CW, Limberger RJ, Rowe N. 2009. The flat-ribbon configuration of the periplasmic flagella of *Borrelia burgdorferi* and its relationship to motility and morphology. *J. Bacteriol.* 191:600–607. <http://dx.doi.org/10.1128/JB.01288-08>.
5. Brandt ME, Riley BS, Radolf JD, Norgard MV. 1990. Immunogenic integral membrane proteins of *Borrelia burgdorferi* are lipoproteins. *Infect. Immun.* 58:983–991.
6. Belisle JT, Brandt ME, Radolf JD, Norgard MV. 1994. Fatty acids of *Treponema pallidum* and *Borrelia burgdorferi* lipoproteins. *J. Bacteriol.* 176:2151–2157.
7. Radolf JD, Bourell KW, Akins DR, Brusca JS, Norgard MV. 1994. Analysis of *Borrelia burgdorferi* membrane architecture by freeze-fracture electron microscopy. *J. Bacteriol.* 176:21–31.
8. Radolf JD, Goldberg MS, Bourell K, Baker SI, Jones JD, Norgard MV. 1995. Characterization of outer membranes isolated from *Borrelia burgdorferi*, the Lyme disease spirochete. *Infect. Immun.* 63:2154–2163.
9. Jones JD, Bourell KW, Norgard MV, Radolf JD. 1995. Membrane topology of *Borrelia burgdorferi* and *Treponema pallidum* lipoproteins. *Infect. Immun.* 63:2424–2434.
10. Ben-Menachem G, Kubler-Kiel J, Coxon B, Yergey A, Schneerson R. 2003. A newly discovered cholesteryl galactoside from *Borrelia burgdorferi*. *Proc. Natl. Acad. Sci. U. S. A.* 100:7913–7918. <http://dx.doi.org/10.1073/pnas.1232451100>.
11. Schröder NW, Schombel U, Heine H, Göbel UB, Zähringer U, Schumann RR. 2003. Acylated cholesteryl galactoside as a novel immunogenic motif in *Borrelia burgdorferi sensu stricto*. *J. Biol. Chem.* 278:33645–33653. <http://dx.doi.org/10.1074/jbc.M305799200>.
12. Stübs G, Fingerle V, Wilske B, Göbel UB, Zähringer U, Schumann RR, Schröder NW. 2009. Acylated cholesteryl galactosides are specific antigens of borrelia causing Lyme disease and frequently induce antibodies in late stages of disease. *J. Biol. Chem.* 284:13326–13334. <http://dx.doi.org/10.1074/jbc.M809575200>.
13. Lin M, Rikihisa Y. 2003. Ehrlichia chaffeensis and Anaplasma phagocytophilum lack genes for lipid A biosynthesis and incorporate cholesterol for their survival. *Infect. Immun.* 71:5324–5331. <http://dx.doi.org/10.1128/IAI.71.9.5324-5331.2003>.
14. Haque M, Hirai Y, Yokota K, Oguma K. 1995. Steryl glycosides: a characteristic feature of the Helicobacter spp.? *J. Bacteriol.* 177:5334–5337.
15. Hirai Y, Haque M, Yoshida T, Yokota K, Yasuda T, Oguma K. 1995. Unique cholesteryl glucosides in *Helicobacter pylori*: composition and structural analysis. *J. Bacteriol.* 177:5327–5333.
16. Smith PF. 1971. Biosynthesis of cholesteryl glucoside by *Mycoplasma gallinarum*. *J. Bacteriol.* 108:986–991.
17. Trott DJ, Alt DP, Zuerner RL, Wannemuehler MJ, Stanton TB. 2001. The search for *Brachyspira* outer membrane proteins that interact with the host. *Anim. Health Res. Rev.* 2:19–30. <http://dx.doi.org/10.1079/AHRR200112>.
18. López D, Kolter R. 2010. Functional microdomains in bacterial membranes. *Genes Dev.* 24:1893–1902. <http://dx.doi.org/10.1101/gad.1945010>.
19. Brown DA, London E. 2000. Structure and function of sphingolipid- and cholesterol-rich membrane rafts. *J. Biol. Chem.* 275:17221–17224. <http://dx.doi.org/10.1074/jbc.R000005200>.
20. London E. 2002. Insights into lipid raft structure and formation from experiments in model membranes. *Curr. Opin. Struct. Biol.* 12:480–486. [http://dx.doi.org/10.1016/S0959-440X\(02\)00351-2](http://dx.doi.org/10.1016/S0959-440X(02)00351-2).
21. Brown RE. 1998. Sphingolipid organization in biomembranes: what physical studies of model membranes reveal. *J. Cell Sci.* 111(Pt 1):1–9.
22. Epan RM. 2008. Proteins and cholesterol-rich domains. *Biochim. Biophys. Acta* 1778:1576–1582. <http://dx.doi.org/10.1016/j.bbame.2008.03.016>.
23. Chen Z, Rand RP. 1997. The influence of cholesterol on phospholipid membrane curvature and bending elasticity. *Bioophys. J.* 73:267–276. [http://dx.doi.org/10.1016/S0006-3495\(97\)78067-6](http://dx.doi.org/10.1016/S0006-3495(97)78067-6).
24. Huttner WB, Zimmerberg J. 2001. Implications of lipid microdomains for membrane curvature, budding and fission. *Curr. Opin. Cell Biol.* 13:478–484. [http://dx.doi.org/10.1016/S0955-0674\(00\)00239-8](http://dx.doi.org/10.1016/S0955-0674(00)00239-8).
25. Nichols B. 2003. Caveosomes and endocytosis of lipid rafts. *J. Cell Sci.* 116:4707–4714. <http://dx.doi.org/10.1242/jcs.00840>.
26. Salaün C, James DJ, Chamberlain LH. 2004. Lipid rafts and the regulation of exocytosis. *Traffic* 5:255–264. <http://dx.doi.org/10.1111/j.1600-0854.2004.0162.x>.
27. LaRocca TJ, Crowley JT, Cusack BJ, Pathak P, Benach J, London E, Garcia-Monco JC, Benach JL. 2010. Cholesterol lipids of *Borrelia burgdorferi* form lipid rafts and are required for the bactericidal activity of a complement-independent antibody. *Cell Host Microbe* 8:331–342. <http://dx.doi.org/10.1016/j.chom.2010.09.001>.
28. LaRocca TJ, Pathak P, Chiantia S, Toledo A, Silvius JR, Benach JL, London E. 2013. Proving lipid rafts exist: membrane domains in the prokaryote *Borrelia burgdorferi* have the same properties as eukaryotic lipid rafts. *PLoS Pathog.* 9:e1003353. <http://dx.doi.org/10.1371/journal.ppat.1003353>.
29. Fraser CM, Casjens S, Huang WM, Sutton GG, Clayton R, Lathigra R, White O, Ketchum KA, Dodson R, Hickey EK, Gwinn M, Dougherty B, Tomb JF, Fleischmann RD, Richardson D, Peterson J, Kerlavage AR, Quackenbush J, Salzberg S, Hanson M, van Vugt R, Palmer N, Adams MD, Gocayne J, Weidman J, Utterback T, Wattley L, McDonald L, Artiach P, Bowman C, Garland S, Fuji C, Cotton MD, Horst K, Roberts K, Hatch B, Smith HO, Venter JC. 1997. Genomic sequence of a Lyme disease spirochaete, *Borrelia burgdorferi*. *Nature* 390:580–586. <http://dx.doi.org/10.1038/37551>.
30. Bergström S, Bundoc VG, Barbour AG. 1989. Molecular analysis of linear plasmid-encoded major surface proteins, OspA and OspB, of the Lyme disease spirochaete *Borrelia burgdorferi*. *Mol. Microbiol.* 3:479–486. <http://dx.doi.org/10.1111/j.1365-2958.1989.tb00194.x>.
31. Benach JL, Coleman JL, Golightly MG. 1988. A murine IgM monoclonal antibody binds an antigenic determinant in outer surface protein A, an immunodominant basic protein of the Lyme disease spirochete. *J. Immunol.* 140:265–272.
32. Schwan TG, Piesman J, Golde WT, Dolan MC, Rosa PA. 1995. Induction of an outer surface protein on *Borrelia burgdorferi* during tick feeding. *Proc. Natl. Acad. Sci. U. S. A.* 92:2909–2913. <http://dx.doi.org/10.1073/pnas.92.7.2909>.
33. Fikrig E, Barthold SW, Kantor FS, Flavell RA. 1990. Protection of mice against the Lyme disease agent by immunizing with recombinant OspA. *Science* 250:553–556. <http://dx.doi.org/10.1126/science.2237407>.
34. Steere AC, Silkand VK, Meurice F, Parenti DL, Fikrig E, Schoen RT, Nowakowski J, Schmid CH, Laukamp S, Buscarino C, Krause DS. 1998. Vaccination against Lyme disease with recombinant *Borrelia burgdorferi* outer-surface lipoprotein A with adjuvant. *Lyme Disease Vaccine Study Group. N. Engl. J. Med.* 339:209–215. <http://dx.doi.org/10.1056/NEJM199807233390401>.
35. Sigal LH, Zahradnik JM, Lavin P, Patella SJ, Bryant G, Haselby R, Hilton E, Kunkel M, Adler-Klein D, Doherty T, Evans J, Molloy PJ, Seidner AL, Sabetta JR, Simon HJ, Klempner MS, Mays J, Marks D, Malawista SE. 1998. A vaccine consisting of recombinant *Borrelia burgdorferi* outer-surface protein A to prevent Lyme disease. *Recombinant Outer-Surface Protein A Lyme Disease Vaccine Study Consortium. N. Engl. J. Med.* 339:216–222. <http://dx.doi.org/10.1056/NEJM199807233390402>.
36. Yang XF, Pal U, Alani SM, Fikrig E, Norgard MV. 2004. Essential role for OspA/B in the life cycle of the Lyme disease spirochete. *J. Exp. Med.* 199:641–648. <http://dx.doi.org/10.1084/jem.20031960>.
37. Connolly SE, Benach JL. 2005. The versatile roles of antibodies in *Borrelia* infections. *Nat. Rev. Microbiol.* 3:411–420. <http://dx.doi.org/10.1038/nrmicro1149>.
38. LaRocca TJ, Holthausen DJ, Hsieh C, Renken C, Mannella CA, Benach JL. 2009. The bactericidal effect of a complement-independent antibody is osmolytic and specific to *Borrelia*. *Proc. Natl. Acad. Sci. U. S. A.* 106:10752–10757. <http://dx.doi.org/10.1073/pnas.0901858106>.
39. Escudero R, Halluska ML, Backenson PB, Coleman JL, Benach JL. 1997. Characterization of the physiological requirements for the bactericidal effects of a monoclonal antibody to OspB of *Borrelia burgdorferi* by confocal microscopy. *Infect. Immun.* 65:1908–1915.
40. Grimm D, Tilly K, Byram R, Stewart PE, Krum JG, Bueschel DM, Schwan TG, Policastro PF, Elias AF, Rosa PA. 2004. Outer-surface protein C of the Lyme disease spirochete: a protein induced in ticks for



- infection of mammals. *Proc. Natl. Acad. Sci. U. S. A.* 101:3142–3147. <http://dx.doi.org/10.1073/pnas.0306845101>.
41. Tilly K, Krum JG, Bestor A, Jewett MW, Grimm D, Bueschel D, Byram R, Dorward D, Vanraden MJ, Stewart P, Rosa P. 2006. *Borrelia burgdorferi* OspC protein required exclusively in a crucial early stage of mammalian infection. *Infect. Immun.* 74:3554–3564. <http://dx.doi.org/10.1128/IAI.01950-05>.
  42. Marconi RT, Samuels DS, Garon CF. 1993. Transcriptional analyses and mapping of the ospC gene in Lyme disease spirochetes. *J. Bacteriol.* 175:926–932.
  43. Earnhart CG, Buckles EL, Dumler JS, Marconi RT. 2005. Demonstration of OspC type diversity in invasive human Lyme disease isolates and identification of previously uncharacterized epitopes that define the specificity of the OspC murine antibody response. *Infect. Immun.* 73:7869–7877. <http://dx.doi.org/10.1128/IAI.73.12.7869-7877.2005>.
  44. Wormser GP, Brisson D, Liveris D, Hanincová K, Sandigursky S, Nowakowski J, Nadelman RB, Ludin S, Schwartz I. 2008. *Borrelia burgdorferi* genotype predicts the capacity for hematogenous dissemination during early Lyme disease. *J. Infect. Dis.* 198:1358–1364. <http://dx.doi.org/10.1086/592279>.
  45. Hanincová K, Mukherjee P, Ogden NH, Margos G, Wormser GP, Reed KD, Meece JK, Vandermause MF, Schwartz I. 2013. Multilocus sequence typing of *Borrelia burgdorferi* suggests existence of lineages with differential pathogenic properties in humans. *PLoS One* 8:e73066. <http://dx.doi.org/10.1371/journal.pone.0073066>.
  46. Onder O, Humphrey PT, McOmber B, Korobova F, Francella N, Greenbaum DC, Brisson D. 2012. OspC is potent plasminogen receptor on surface of *Borrelia burgdorferi*. *J. Biol. Chem.* 287:16860–16868. <http://dx.doi.org/10.1074/jbc.M111.290775>.
  47. Lagal V, Portnoï D, Faure G, Postic D, Baranton G. 2006. *Borrelia burgdorferi* sensu stricto invasiveness is correlated with OspC-plasminogen affinity. *Microbes Infect.* 8:645–652. <http://dx.doi.org/10.1016/j.micinf.2005.08.017>.
  48. Coleman JL, Sellati TJ, Testa JE, Kew RR, Furie MB, Benach JL. 1995. *Borrelia burgdorferi* binds plasminogen, resulting in enhanced penetration of endothelial monolayers. *Infect. Immun.* 63:2478–2484.
  49. Stewart PE, Wang X, Bueschel DM, Clifton DR, Grimm D, Tilly K, Carroll JA, Weis JJ, Rosa PA. 2006. Delineating the requirement for the *Borrelia burgdorferi* virulence factor OspC in the mammalian host. *Infect. Immun.* 74:3547–3553. <http://dx.doi.org/10.1128/IAI.00158-06>.
  50. Yang X, Promnares K, Qin J, He M, Shroder DY, Kariu T, Wang Y, Pal U. 2011. Characterization of multiprotein complexes of the *Borrelia burgdorferi* outer membrane vesicles. *J. Proteome Res.* 10:4556–4566. <http://dx.doi.org/10.1021/pr200395b>.
  51. Crowley JT, Toledo AM, LaRocca TJ, Coleman JL, London E, Benach JL. 2013. Lipid exchange between *Borrelia burgdorferi* and host cells. *PLoS Pathog.* 9:e1003109. <http://dx.doi.org/10.1371/journal.ppat.1003109>.
  52. García Moncá JC, Wheeler CM, Benach JL, Furie RA, Lukehart SA, Stanek G, Steere AC. 1993. Reactivity of neuroborreliosis patients (Lyme disease) to cardiolipin and gangliosides. *J. Neurol. Sci.* 117:206–214. [http://dx.doi.org/10.1016/0022-510X\(93\)90175-X](http://dx.doi.org/10.1016/0022-510X(93)90175-X).
  53. Coleman JL, Crowley JT, Toledo AM, Benach JL. 2013. The HtrA protease of *Borrelia burgdorferi* degrades outer membrane protein BmpD and chemotaxis phosphatase CheX. *Mol. Microbiol.* 88:619–633. <http://dx.doi.org/10.1111/mmi.12213>.
  54. Silviu JR. 2003. Fluorescence energy transfer reveals microdomain formation at physiological temperatures in lipid mixtures modeling the outer leaflet of the plasma membrane. *Biophys. J.* 85:1034–1045. [http://dx.doi.org/10.1016/S0006-3495\(03\)74542-1](http://dx.doi.org/10.1016/S0006-3495(03)74542-1).
  55. Sadziene A, Wilske B, Ferdows MS, Barbour AG. 1993. The cryptic ospC gene of *Borrelia burgdorferi* B31 is located on a circular plasmid. *Infect. Immun.* 61:2192–2195.
  56. Eicken C, Sharma V, Klabunde T, Owens RT, Pikas DS, Höök M, Sacchettini JC. 2001. Crystal structure of Lyme disease antigen outer surface protein C from *Borrelia burgdorferi*. *J. Biol. Chem.* 276:10010–10015. <http://dx.doi.org/10.1074/jbc.M010062200>.
  57. Kumaran D, Eswaramoorthy S, Luft BJ, Koide S, Dunn JJ, Lawson CL, Swaminathan S. 2001. Crystal structure of outer surface protein C (OspC) from the Lyme disease spirochete, *Borrelia burgdorferi*. *EMBO J.* 20:971–978. <http://dx.doi.org/10.1093/emboj/20.5.971>.
  58. Lenhart TR, Akins DR. 2010. *Borrelia burgdorferi* locus BB0795 encodes a BamA orthologue required for growth and efficient localization of outer membrane proteins. *Mol. Microbiol.* 75:692–709. <http://dx.doi.org/10.1111/j.1365-2958.2009.07015.x>.
  59. Chen S, Kumru OS, Zückert WR. 2011. Determination of borrelia surface lipoprotein anchor topology by surface proteolysis. *J. Bacteriol.* 193:6379–6383. <http://dx.doi.org/10.1128/JB.05849-11>.
  60. Pal U, Yang X, Chen M, Bockenstedt LK, Anderson JF, Flavell RA, Norgard MV, Fikrig E. 2004. OspC facilitates *Borrelia burgdorferi* invasion of *Ixodes scapularis* salivary glands. *J. Clin. Invest.* 113:220–230. <http://dx.doi.org/10.1172/JCI200419894>.
  61. Liang FT, Jacobs MB, Bowers LC, Philipp MT. 2002. An immune evasion mechanism for spirochetal persistence in Lyme borreliosis. *J. Exp. Med.* 195:415–422. <http://dx.doi.org/10.1084/jem.20011870>.
  62. Tilly K, Bestor A, Dulebohn DP, Rosa PA. 2009. OspC-independent infection and dissemination by host-adapted *Borrelia burgdorferi*. *Infect. Immun.* 77:2672–2682. <http://dx.doi.org/10.1128/IAI.01193-08>.
  63. Tilly K, Bestor A, Rosa PA. 2013. Lipoprotein succession in *Borrelia burgdorferi*: similar but distinct roles for OspC and VlsE at different stages of mammalian infection. *Mol. Microbiol.* 89:216–227. <http://dx.doi.org/10.1111/mmi.12271>.
  64. Battisti JM, Bono JL, Rosa PA, Schrupf ME, Schwan TG, Policastro PF. 2008. Outer surface protein A protects Lyme disease spirochetes from acquired host immunity in the tick vector. *Infect. Immun.* 76:5228–5237. <http://dx.doi.org/10.1128/IAI.00410-08>.
  65. Coleman JL, Benach JL. 1992. Characterization of antigenic determinants of *Borrelia burgdorferi* shared by other bacteria. *J. Infect. Dis.* 165:658–666. <http://dx.doi.org/10.1093/infdis/165.4.658>.
  66. Coleman JL, Rogers RC, Benach JL. 1992. Selection of an escape variant of *Borrelia burgdorferi* by use of bactericidal monoclonal antibodies to OspB. *Infect. Immun.* 60:3098–3104.
  67. Earnhart CG, Leblanc DV, Alix KE, Desrosiers DC, Radolf JD, Marconi RT. 2010. Identification of residues within ligand-binding domain 1 (LBD1) of the *Borrelia burgdorferi* OspC protein required for function in the mammalian environment. *Mol. Microbiol.* 76:393–408. <http://dx.doi.org/10.1111/j.1365-2958.2010.07103.x>.
  68. Toledo A, Coleman JL, Kuhlow CJ, Crowley JT, Benach JL. 2012. The enolase of *Borrelia burgdorferi* is a plasminogen receptor released in outer membrane vesicles. *Infect. Immun.* 80:359–368. <http://dx.doi.org/10.1128/IAI.05836-11>.
  69. Frank KL, Bundle SF, Kresge ME, Eggers CH, Samuels DS. 2003. aadA confers streptomycin resistance in *Borrelia burgdorferi*. *J. Bacteriol.* 185:6723–6727. <http://dx.doi.org/10.1128/JB.185.22.6723-6727.2003>.
  70. Blish EG, Dyer WJ. 1959. A rapid method of total lipid extraction and purification. *Can. J. Biochem. Physiol.* 37:911–917. <http://dx.doi.org/10.1139/o59-099>.
  71. Kiskowski MA, Hancock JF, Kenworthy AK. 2009. On the use of Ripley's K-function and its derivatives to analyze domain size. *Biophys. J.* 97:1095–1103. <http://dx.doi.org/10.1016/j.bpj.2009.05.039>.
  72. Ripley BD. 1979. Test of randomness for spatial point patterns. *J. R. Stat. Soc. Series B Stat. Methodol.* 41:368–374.
  73. Ripley BD. 1977. Modelling spatial patterns. *J. R. Stat. Soc. Series B Stat. Methodol.* 39:172–212.